

# Numerical Simulation of Buoyant Plume Dispersion in a Stratified Atmosphere Using a Lagrangian Stochastic Model

**Hyun-Goo Kim\***

*Research Institute of Industrial Science and Technology, Pohang, Kyungbuk 790-330, Korea*

**Yoo-Jeong Noh**

*Department of Meteorology, Florida State University, U.S.A.*

**Choung-Mook Lee, Don-Bum Choi**

*Pohang University of Science and Technology, Pohang, Kyungbuk 790-784, Korea*

In the present paper, numerical simulations of buoyant plume dispersion in a neutral and stable atmospheric boundary layer have been carried out. A Lagrangian Stochastic Model (LSM) with a Non-Linear Eddy Viscosity Model (NLEVM) for turbulence is used to generate a Reynolds stress field as an input condition of dispersion simulation. A modified plume-rise equation is included in dispersion simulation in order to consider momentum effect in an initial stage of plume rise resulting in an improved prediction by comparing with the experimental data. The LSM is validated by comparing with the prediction of an Eulerian Dispersion Model (EDM) and by the measured results of vertical profiles of mean concentration in the downstream of an elevated source in an atmospheric boundary layer. The LSM predicts accurate results especially in the vicinity of the source where the EDM underestimates the peak concentration by 40% due to inherent limitations of gradient diffusion theory. As a verification study, the LSM simulation of buoyant plume dispersions under a neutral and stable atmospheric condition is compared with a wind-tunnel experiment, which shows good qualitative agreements.

**Key Words :** Buoyant Plume Dispersion, Lagrangian Stochastic Model (LSM), Non-Linear Eddy Viscosity Model (NLEVM)

## 1. Introduction

An accurate prediction of dispersion behavior of buoyant plume in a stratified atmosphere has a close relation to various environmental problems. This is because an analytical prediction tool, which enables the effect of emission of atmospheric pollutants around the emission source to be analyzed quantitatively, can contribute significantly to an assessment of environmental con-

ditions. Such a tool would lead to an establishment of criteria for environmental impact evaluation of facilities emitting various atmospheric pollutants and of atmospheric pollution-related policies and regulations. Furthermore, since the emission of atmospheric pollutants from a factory zone or an incineration plant directly affects health of local residents, the demand for accurate pollution assessment of a local zone is ever increasing.

Factors affecting plume dispersion are emission conditions such as buoyancy and momentum of the emitted plume, atmospheric wind direction and speed, conditions of thermal stratification, terrain and ground structures. Actually, these conditions should be combined to find complicated dispersion patterns. Among them, the buoyancy is

---

\* Corresponding Author,  
E-mail : hyungoo@rist.re.kr  
TEL : +82-54-279-6615; FAX : +82-54-279-6239  
Research Institute of Industrial Science and Technology,  
Pohang, 790-330, Korea (Manuscript Received August  
14, 2002; Revised November 16, 2002)

a major mechanism dominating a plume motion, and it affects plume-rise and dispersion patterns. Plume emitted from a stack shows various dispersion behaviors such as looping, coning, fanning, fumigation and lofting depending upon the thermal stratification condition of the atmosphere. Accordingly, a ground-level concentration of plume can show a variety of different profiles depending upon the stratification condition. Since a significant change in temperature and atmospheric condition can occur during a day, it is necessary to include the stratified-atmosphere condition in the prediction of plume dispersion.

Recently, some attempts to carry out numerical simulation of plume dispersion using the Lagrangian Stochastic Model (LSM or Lagrangian Dispersion Model; LDM) have been made. The Langevin equation used in the LSM for simulation of a random walk of particles in a turbulent flow field has an advantage in representing properly the various statistical characteristics of a turbulent flow (Thomson, 1987, van Dop et al., 1985). Plume dispersion takes place by atmospheric flow as an advection and dispersion medium, and therefore the analysis of the atmospheric flow field has to precede the prediction of plume dispersion. In the prediction of the atmospheric flow field via the Reynolds averaged Navier-Stokes equation, a proper turbulence modeling becomes an important factor. As a usual practice, the turbulence model had been most frequently used in the prediction of an atmospheric flow. In an effort to improve the turbulence modeling, Kim and Patel (2000) proposed a method for decomposing actual atmospheric anisotropic Reynolds stresses by using a non-linear eddy viscosity model (NLEVM). They made extensive comparative studies of various typical turbulent flow models for the atmospheric flow passing over a complex terrain, and proposed a better method for turbulence modeling.

In the present study, numerical predictions of buoyant plume dispersion in two different cases of atmospheric boundary layer i.e. neutral and stable cases are made by using the LSM. A non-linear eddy viscosity model is applied to the Reynolds stresses in the Navier-Stokes equation

which is used for the numerical simulation of buoyant plume dispersion. In order to verify the reliability of the numerical model, it is compared with the result of the buoyant plume dispersion experiment conducted in a thermally stratified wind-tunnel by Kim et al. (1997). In addition, a modified plume-rise equation is included in the LSM in order to account the momentum effect on the plume rise in an initial stage.

## 2. Numerical Methods

### 2.1 Numerical model of atmospheric flow field

An analysis of the neutral and stable atmospheric boundary layers is carried out. The energy equation is added to account for thermal stratification effect of an atmospheric flow to the method reported in the authors' previous paper (Kim and Lee, 1998) which assumed a neutral atmospheric boundary layer. The governing equations of an incompressible atmospheric flow in the thermal stratification are the continuity, momentum and energy equations, which are shown below with the conventional indices notations :

$$\begin{aligned} U_{i,j} &= 0 \\ (U_i U_j)_{,j} + p_{,i} / \rho - (\nu U_{i,j} - \overline{u_i u_j})_{,j} \\ &= -2\varepsilon_{ijk} \omega_j U_k - \alpha (\Theta - \Theta_a) g_i \\ (U_i \Theta)_{,i} - (\nu_t \Theta_{,i} / \sigma_\theta)_{,i} &= 0 \end{aligned} \quad (1)$$

Here,  $x_i = (x, y, z)$  represents the right-handed Cartesian coordinates with  $x$  in the wind direction and  $z$  in vertically upward direction,  $U_i$  and  $u_i$  the mean velocity and the fluctuation velocity,  $\rho$  and  $\nu$  the air density and the kinematic viscosity,  $\Theta$  and  $\Theta_a$  the plume and atmospheric temperature,  $\alpha$  the adiabatic expansion coefficient, and  $g_i = -g\delta_{i3}$  the gravitational acceleration vector and  $\omega_i$  the angular velocity vector of earth rotation,  $\nu_t = C_\mu k^2 / \varepsilon$  the turbulent eddy viscosity, and  $\sigma_\theta$  the Prandtl-Schmitt number for thermal diffusion.

In order to integrate the foregoing equations, the Reynolds stresses  $-\overline{u_i u_j}$  should be modeled in terms of the mean velocity gradients. The frequently used model is the so called  $k-\varepsilon$  model

which assumes an isotropic turbulence and defines the Reynolds stresses by

$$-\overline{u_i u_j} = 2\nu_t S_{ij} - \frac{2}{3} k \delta_{ij} \quad (2)$$

where  $S_{ij}$  denotes the mean strain tensor given by  $(U_{i,j} + U_{j,i})/2$ . The turbulent eddy viscosity is obtained from the following turbulence kinetic energy ( $k = \overline{u_i u_i}/2$ ) and turbulence kinetic energy dissipation rate ( $\epsilon$ ) equation:

$$\begin{aligned} (U_i k)_{,i} - (\nu_t k_{,i} / \sigma_k)_{,i} \\ = -\overline{u_i u_j} S_{ij} - \epsilon + \alpha g_i \Theta_{,i} \frac{\nu_t}{\sigma_\theta} \\ (U_i \epsilon)_{,i} - (\nu_t \epsilon_{,i} / \sigma_\epsilon)_{,i} \\ = -\left( C_1 \overline{u_i u_j} S_{ij} + C_2 \epsilon + C_1 C_3 \alpha g_i \Theta_{,i} \frac{\nu_t}{\sigma_\theta} \right) \frac{\epsilon}{k} \end{aligned} \quad (3)$$

where  $\sigma_k$  and  $\sigma_\epsilon$  are the turbulence constants associated with  $k$  and  $\epsilon$ , respectively.

In all of the atmospheric flow simulations presented here, the numerical methods of Kim and Lee (1998) and Kim and Patel (2000) are used with appropriate computational grids, terrain roughness and boundary conditions.

Detering and Etling (1985), Duykerke (1988) applied modified turbulence constants in order to consider the effect of the Coriolis force in the numerical simulations of the neutral and stable atmospheric boundary layers. However in the present study, the standard  $k-\epsilon$  turbulence model is used since the effect of the Coriolis force is negligible at the lower atmospheric boundary layer. The model constants used here are  $C_\mu = 0.09$ ,  $C_1 = 1.44$ ,  $C_2 = 1.92$ ,  $C_3 = 1.0$  (unstable) or 0.2 (stable),  $\sigma_k = 1.0$ ,  $\sigma_\epsilon = 1.3$ , and  $\sigma_\theta = 0.74$ .

If the modeling of the Reynolds stresses is confined to the order of a linear function of  $S_{ij}$ , the characteristics of the turbulent flow becomes linear and isotropic, and furthermore, if the atmospheric boundary layer is stationary, then,  $S_{ij} = 0$  except  $S_{33}$ . Therefore, the values of respective directional normal Reynolds stresses should be identical i.e.  $\overline{uu} = \overline{vv} = \overline{ww}$ .

In reality, even in the stationary atmospheric boundary layer, it is well known from the experimental result of Counihan (1975) that the following proportion exists between the normal Reynolds stresses:

$$\sqrt{\overline{uu}} = \sqrt{\overline{vv}} = \sqrt{\overline{ww}} = 1.0 : 0.8 : 0.52 \quad (4)$$

In the present investigation, the Reynolds stresses are decomposed by using the following NLEVM from the method suggested by Kim and Patel (2000):

$$\begin{aligned} -\overline{u_i u_j} = & 2\nu_t S_{ij} - \frac{2}{3} k \delta_{ij} \\ & + C_I \nu_t \frac{k}{\epsilon} \left( S_{jk} S_{ki} - \frac{1}{3} S_{kl} S_{kl} \delta_{ij} \right) \\ & + C_{II} \nu_t \frac{k}{\epsilon} (\Omega_{jk} S_{kj} + \Omega_{jk} S_{ki}) \\ & + C_{III} \nu_t \frac{k}{\epsilon} \left( \Omega_{jk} \Omega_{jk} - \frac{1}{3} \Omega_{ljk} \Omega_{lk} \delta_{ij} \right) \\ & + C_{IV} C_\mu \nu_t \frac{k^2}{\epsilon^2} \left( S_{ki} \Omega_{lj} + S_{kj} \Omega_{li} - \frac{2}{3} S_{km} \Omega_{lm} \delta_{ij} \right) S_{kl} \\ & + C_{VII} C_\mu \nu_t \frac{k^2}{\epsilon^2} S_{ij} S_{kl} S_{kl} + C_{VII} C_\mu \nu_t \frac{k^2}{\epsilon^2} S_{ij} \Omega_{kl} \Omega_{kl} \end{aligned} \quad (5)$$

Here,  $\Omega_{ij} = (U_{i,j} - U_{j,i})/2$  represents the rotational mean vorticity tensor,  $C_I \sim C_{VII}$  represent the turbulence constants of nonlinear stresses (Craft, 1997),  $C_I \sim C_{III}$  correspond to the quadratic anisotropic normal stress terms, and  $C_{IV} \sim C_{VII}$  represent the cubic terms related to the nonlinear stresses caused by streamline curvature and rotation. Then, the atmospheric flow field is computed using the Reynolds stresses given by Eq. (5) and these Reynolds stresses are used as an input for the analysis of plume dispersion.

It should be noted here that atmospheric flow and dispersion simulation are decoupled in the present study under the assumption that the plume rise would not disturb atmospheric flow seriously (Anfossi et al., 1993).

## 2.2 Numerical model of plume dispersion

The LSM is a dispersion model for simulating a random turbulent motion of particles in the turbulent flow field under the assumption that the plume should be represented as a set of many particles. The plume concentration field is then calculated from the stochastic analysis of the distribution of these particles. In a three dimensional space, a position of plume particles ( $X_i$ ) after a small time step ( $\Delta t$ ) from any time ( $t$ ) is determined by the following equation:

$$X_i(t + \Delta t) = X_i(t) + (U_i + u_i + w_b \delta_{3i}) \cdot \Delta t \quad (6)$$

where  $w_b$  represents the buoyant plume-rise velocity which will be described in detail in Section 2.3. The turbulent velocity of a plume particle is expressed on the basis of the Langevin equation indicating a random motion of particles (van Dop et al., 1985) by

$$u_i(t+\Delta t) = R_i(t) u_j(t) \delta_{ij} + (\sigma_i \gamma_i \delta_{ij} + T_3 \sigma_{3,3}^2 \delta_{33}) \cdot \sqrt{1-R_i^2(t)} \quad \text{for } i=1, 2, 3 \quad (7)$$

Here,  $\gamma_i$  represents a random number vector,  $\sigma_i = \sqrt{u_i u_i}$  represents a root-mean-square turbulent velocity calculated by Eq. (5) and  $R_i(\tau) = \exp(-\tau/T_i)$  is an autocorrelation function of the turbulent flow velocity ( $u_i$ ) under the assumption that it should be of an exponential form. In the present study, the Lagrangian time scale ( $T_i$ ) expressed as a function of eddy turnover time is used to account for anisotropic characteristics of turbulence influenced by local topography (Lu, 1995).

$$T_i = C_T \frac{2}{3} \frac{\sigma_i}{\epsilon}; \quad C_T = 0.212 \quad (8)$$

In Eq. (7), since a horizontal movement of plume particles is dominantly made through advection by the mean flow, the turbulent flow velocity ( $u = u_i$ ) may be assumed negligible. However, when the mean flow velocity becomes small near the ground, the magnitude of the turbulent flow velocity component being of the same order of that of the mean velocity should not be ignored, and therefore, it is retained in the present analysis of plume dispersion. The boundary condition employed in this work is at the ground where perfect reflection of displacement and velocity of a particle are assumed.

The first term in the right-hand side of Eq. (7) is a term representing reduction of a particle velocity caused by interaction between particles and the ambient atmosphere. An initial velocity of collagen particles in the Brownian motion is damped by the friction with ambient fluid. The second term represents a micro velocity change caused by a random motion of particles. The third term represents perturbation of the vertical turbulence velocity in the time duration of  $\Delta t$ .

### 2.3 Numerical model of buoyant plume rise

The 2/3-law plume-rise equation of Briggs (1975) was introduced, as suggested by Anfossi et al. (1993), to describe a vertical velocity component of plume-rise caused by buoyancy and momentum. Particularly, the effect of the initial momentum of plume emitted from a stack was fully considered in the present numerical model including the condition of atmospheric stability. Such a consideration is useful in validating numerical results by wind-tunnel experiments. In case of a plume-rise experiment on a laboratory scale, a substantial initial plume momentum is required in order to prevent the instant scattering of plume right after its emission from a stack.

The following is an equation for calculating the vertical velocity component of the plume dispersion in which the effect of the atmospheric stability on the plume-rise at the final phase is included by a curve fitting of plume rise equations for initial and final phases.

$$w_b = \frac{Z_b(t+\Delta t) - Z_b(t)}{\Delta t}$$

$$Z_b = Z_i \left[ 1 + 2.6^{-2} \left( \frac{sU}{F_b} \right)^{2/3} Z_i^2 \right]^{-1/2} \quad (9)$$

$$Z_i = 3^{1/3} \left( \frac{F_b}{2\beta^2 U} x^2 + \frac{F_m}{\beta'^2 U^2} x \right)^{1/3}$$

Here,  $Z_i$  is a term representing an initial plume-rise,  $U = U_1$ ,  $F_b$  the buoyant flux parameter, and  $F_m$  the momentum flux parameter which are defined as follows:

$$F_b = g w_s \gamma^2 (\Theta - \Theta_a) / \Theta_s \quad (10)$$

$$F_m = w_s^2 \gamma^2 \Theta_a / \Theta_s$$

in which,  $\gamma$  represents the radius of stack,  $w_s$  the emission velocity of the plume,  $\Theta_a$ ,  $\Theta_s$  the absolute temperature of the atmosphere and the plume, respectively,  $s = ag(\partial\Theta_a/\partial z)$  the stability parameter which has a positive value in a stable condition and zero in a neutral condition. In Eq. (9), the value of the buoyant entrainment coefficient ( $\beta$ ) is taken as 0.6 which was reported by Briggs (1975) and the coefficient of entrainment caused by the plume momentum ( $\beta'$ ) is obtained by  $\beta' = 0.4(1 + 0.3U/w_s)$  which was suggested by Willis and Deardorff (1983).

Since plume particles have characteristics of the turbulent flow, and are defined in the form of

$$F_b^j = \overline{F_b} + F_b^* \quad (j=1, 2, \dots, N) \quad (11)$$

$$F_m^j = \overline{F_m} + F_m^*$$

where the upper bar means an ensemble average in respect of the number of particles ( $N$ ) and the prime means a small random fluctuation. As reported in Anfossi et al. (1993) on wind-tunnel measurements, the plume particles are assumed to have a random fluctuation with standard deviation by one-third of the mean value.

### 3. Results and Discussion

#### 3.1 Analysis of atmospheric flow in a neutral or stable condition

The results of numerical analysis of the neutral or stable atmospheric boundary layer are validated by comparing with the theoretical results based on the law of similarity of Monin-Obukhov (1954), which was often used as a standard of comparison in the study on the atmospheric boundary layer, and the empirical formula introduced by Brost and Wynaard (1978) for the turbulent eddy viscosity in the stratified atmospheric boundary layer which is given by

$$\frac{\nu_t}{\chi u_* \delta} = \frac{z}{\delta} \left(1 - \frac{z}{\delta}\right)^{1.5} \phi_m^{-1}(z/L) \quad (12)$$

where  $\chi$  represents the von Karman coefficient,  $u_*$  the friction velocity,  $\delta$  the height of the boundary layer and  $\phi_m$  is the similarity function of Monin-Obukhov which is expressed by the following empirical formula

$$\phi_m(z/L) = \frac{\chi z}{u_*} \left(\frac{\partial U}{\partial z}\right) = 1 + 4.7 \frac{z}{L} \quad (13)$$

where  $L = u_*^2 / (\chi a g \theta_*)$  is a length scale of Monin-Obukhov and  $\theta_* = -(\overline{w\theta})|_{z=0} / u_*$ . For the stable condition  $L$  has a positive value, and for the neutral condition, it diverges to infinity. Therefore, in the neutral condition,  $\phi_m$  converges to 1.

Figure 1 shows the vertical profiles of mean flow velocity and turbulent eddy viscosity in the atmospheric boundary layer which are calculated for both neutral and stable atmospheric con-

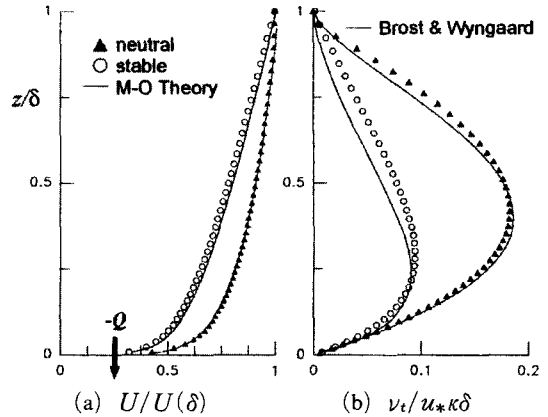


Fig. 1 Vertical profiles of (a) mean horizontal velocity and (b) turbulent eddy viscosity in neutral and stable atmospheric boundary layers (symbols : present computations, lines : empirical predictions)

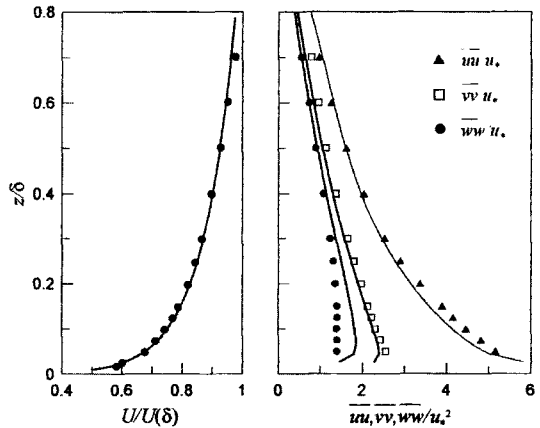


Fig. 2 Vertical profiles of (a) mean horizontal velocity and (b) normal Reynolds stresses in neutral atmospheric boundary layer (symbols : measurements, lines : NLEVM predictions)

ditions together with those calculated by the Monin-Obukhov theory for the mean velocity and by Eq. (12) for the eddy viscosity. The results of the numerical simulation are well in agreement with the results of the aforesaid formulas of Monin-Obukhov and Brost-Wynaard.

Figure 2 shows the measured results of normal Reynolds stresses in a stable atmospheric boundary layer and the calculated results using the NLEVM. It is confirmed that the characteristics

of an anisotropic turbulent flow in the actual atmospheric boundary layer could be simulated adequately by the NLEVM.

**3.2 Analysis of plume dispersion in neutral atmospheric boundary layer**

Figure 3 is shown to compare the results of numerical analysis of plume dispersion in a neutral atmospheric boundary layer with the wind-tunnel results of Raupach and Legg (1983) and the results of the Eulerian Dispersion Model (EDM) of Kim and Lee (1998). The vertical concentration profiles are shown at the downwind distances of  $x/H_s=2.5, 7.5, 15$  where  $H_s$  is the height of an emission source. The plume concentration is shown in dimensionless values of  $CU_sH_s/Q$  where  $C$  is the concentration,  $U_s$  the uniform horizontal wind velocity in the upstream and  $Q$  the emission rate per unit time at the height of the elevated emission source.

In Fig. 3, the result of numerical analysis of LSM as indicated in solid lines shows a high concentration at  $x/H_s=2.5$  at the emission-source elevation in agreement with the measured results, while the result of the EDM in dashed lines shows a much lower peak value. This implies that the LSM is free from the error associated with the gradient diffusion theory (K-theory) used in the EDM.

In Fig. 3(b) and (c), ripples are found in the concentration profiles predicted by LSM, and it

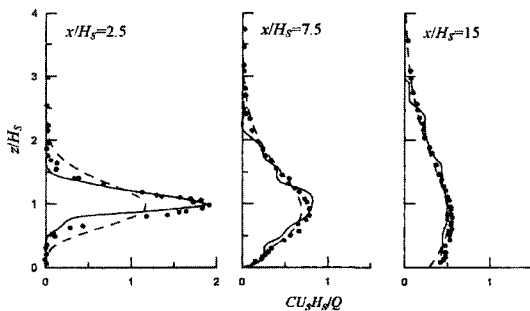


Fig. 3 Comparisons of vertical profiles of mean concentration from an elevated plume source in a neutral atmospheric boundary layer (solid lines : LSM, dashed lines : EDM, symbols : measurements)

is thought that this is due to insufficient number of particles used in the simulation (20,000 particles per second). Identical to the real dispersion experiments where long-term average is required to obtain smoothly averaged concentration profiles, LSM simulation also requires enough number of particles and Fig. 3 reflects this fact clearly.

Furthermore, the discretization method of convection term in the EDM and the choice of the mesh size can be major source of such a discrepancy in the results, while the LSM is independent of numerical grid and discretization method in calculating the position of a plume particle and therefore, the LSM is less subject to the errors resulting from the theoretical modeling of the plume diffusion and numerical schemes.

**3.3 Analysis of buoyant plume dispersion in neutral atmospheric boundary layer**

Figure 4 shows a comparison of buoyant plume rising trajectory in neutral atmospheric boundary layer with the experimental results of Huq and Stewart (1996). It shows that the present LSM prediction (solid line) for which the modified equation i. e. Eq. (9) is used is more adequate in comparison with the LSM method of Briggs (dotted line) for the distance of  $z/l_b$  less than 100. In Fig. 4,  $l_b=F_b/U^3$  represents a buoyancy length scale. In case of a high emission rate as in a power plant, the rising effect caused by an initial momentum of plume can last to the final

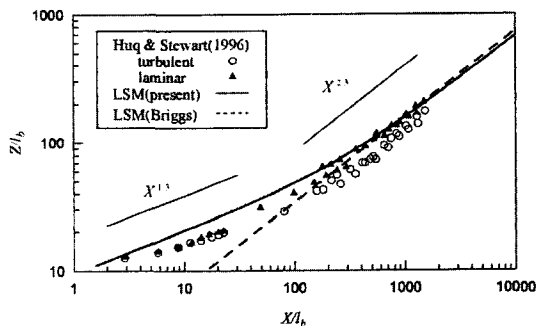


Fig. 4 Comparison of plume mean trajectories (symbols : experiments, solid line : LSM with the modified plume rise equation, dashed line : LSM with the original Briggs equation)

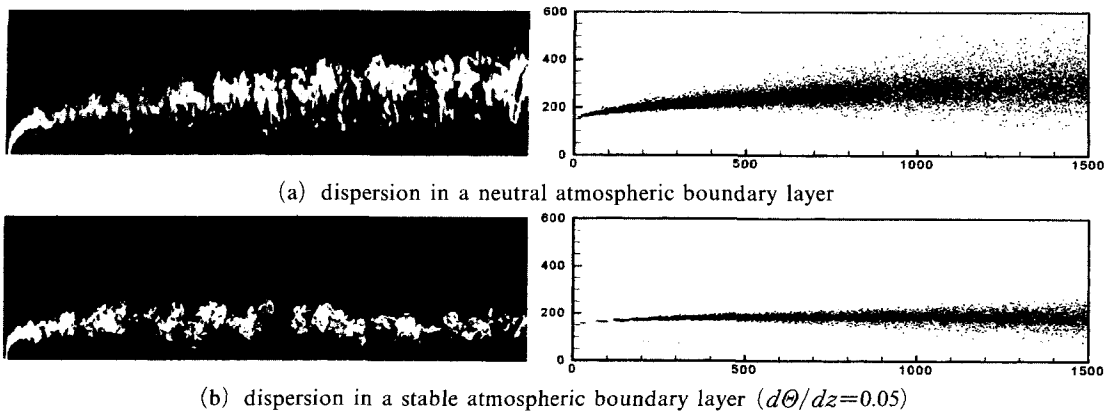


Fig. 5 Comparisons of buoyant plume dispersion patterns of the wind-tunnel experiments with the present LSM simulations shown on the right-hand side

phase in the plume trajectory, and, therefore, the modified equation as suggested in the present investigation would be a more appropriate tool to be used in the prediction of plume dispersion.

### 3.4 Analysis of plume dispersion in stable atmospheric boundary layer

The LSM was applied to numerical simulations of buoyant plume dispersion in neutral and stable atmospheric boundary layers. The results are compared with the visualized results of the plume dispersion experiment conducted in a thermally stratified wind tunnel by Kim et al. (1997). They generated an atmospheric boundary layer under various stratified atmospheric conditions, and thereby observed various dispersion processes of buoyant plume emitted from a stack. The comparison given in Fig. 5 shows similar plume dispersion behaviors. It can be observed that in the neutral atmospheric boundary layer an ideal plume dispersion which has a monotonically rising behavior with broader dispersion, while in the stable atmospheric boundary layer the plume-dispersion breadth and the mean plume-rising height are found to be much smaller than those in the neutral atmospheric boundary layer. Such a phenomenon can be explained from the fact that a stable temperature gradient ( $\partial\theta_a/\partial z > 0$ ) suppress the turbulence and the buoyancy growth in plume dispersion resulting in reduction of the plume rising height and the plume dispersion breadth. This suggests that if a low

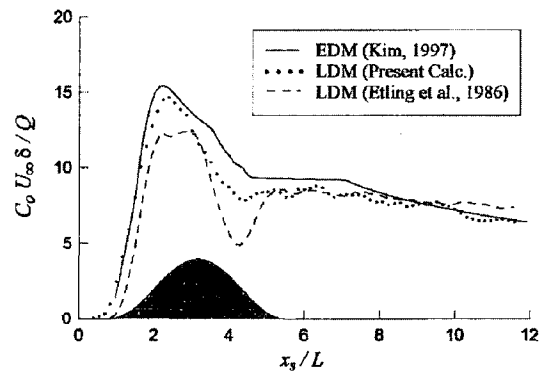
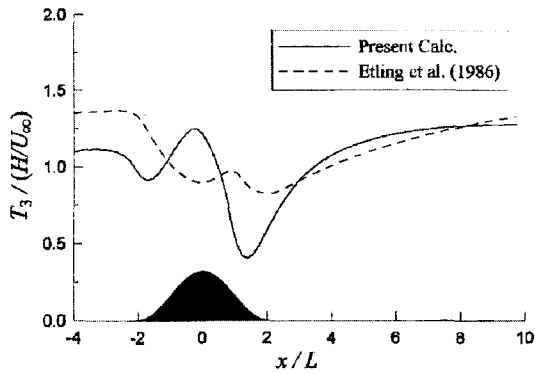


Fig. 6 Comparison of the ground-level concentration by different dispersion models over hilly terrain from the elevated line source at hill front (solid line: EDM, dotted line: LSM, dashed line: LSM by Etling et al., 1986)

stack emits plumes in a stable atmospheric boundary layer, there could be a good probability of high ground concentration of air pollutants in the path of plume dispersion.

### 3.5 Analysis of plume dispersion over hilly terrain

As a final stage of the present study, the LSM simulation of plume dispersion over hilly terrain is carried out. Kim and Lee (1998) have simulated atmospheric flows over hilly terrain and showed good agreements from comparisons with their wind-tunnel experiments. In the present simulation, therefore, the computational result of Kim and Lee (1998) is used as a carrier flow field



**Fig. 7** Distribution of the Lagrangian timescale  $T_3$  over hilly terrain at the height of emission source (solid line: LSM, dashed line: LSM by Etling et al., 1986)

of plume dispersion, and the prediction of the present LSM is compared with their EMD result for the same situation.

Figure 6 shows the distributions of ground-level concentration (GLC) over a single hill where the emission source is located at hill front with one-quarter height of hill height, i.e.,  $H_s = 0.25H$ . This situation corresponds to dispersion in complex terrain ( $H_s < H$ ). Generally, the results of the present LSM and the EDM by Kim and Lee (1998) are in good agreement; almost the same peak values and identical shape of distribution. It is deduced that the phase shift of GLC distribution between two models shown in Fig. 6 is originated in approximation of point source to a finite volume source in the EDM.

In Fig. 6, it is noted that the result of the LSM by Etling et al. (1986) shows noticeable under-prediction of GLC in the leeward side of the hill compared with the results of the other models. Figure 7 shows the comparison of the distributions of Lagrangian timescales between the present LSM and the LSM of Etling et al. (1986). It shows that the Lagrangian timescale calculated by the present LSM has a dip down at leeward slope of the hill but the mixing length model used by Etling et al. (1986) does not. In the leeward slope, the turbulence intensity increases by the velocity deficit in the wake region which implies that the Lagrangian time scale should be smaller. Thus, the Lagrangian time scale based on Eq. (8)

is deemed more adequate compared to the method of mixing length model in the complex terrain.

## 4. Conclusion

In the present investigation, the plume-rise equation is modified so that the plume rising effect caused by the initial momentum of plume emitted from a stack can be taken into account using a Lagrangian stochastic model. The results are qualitatively verified by comparing with the laboratory experiments which was conducted with a high initial emission velocity of plume. The atmospheric boundary layer flow in a stratified atmosphere is calculated by using the anisotropic Reynolds stresses in the Navier-Stokes equation. The flow field thus obtained is used in the numerical simulation of buoyant plume dispersion. This method is anticipated to be extended to a numerical simulation of buoyant plume dispersion in a complex terrain in the future, which will be free from undesirable uncertainties arising from using an empirical formula for calculating the turbulent flow characteristics in atmospheric boundary layer.

It goes without saying, a continuous improvement of the numerical model verified quantitatively by reliable laboratory experiments should be carried out in order to provide a reliable prediction method of atmospheric pollutant dispersion over complex terrain. In the meantime, a sample application of the LSM for a single hill of mild slope demonstrated and the effectiveness of NLEVM to calculate Lagrangian timescale is shown.

## Acknowledgment

This work was supported by the BK21 program of Ministry of Education and Human Resources of Republic of Korea, the National Research Laboratory program by Ministry of Science and Technology, and Air Protection Research Team of Research Institute of Industrial Science and Technology. The authors would like to extend their gratitude to Prof. Kyung-Cheon Kim and Dr. Byung-Chan Kim of Pusan National Univer-



sity for offering their visualized results of the wind tunnel experiment of plume dispersion in a stratified atmosphere.

## References

- Anfossi, D., Ferrero, E., Brusasca, G., Tinarelli, G., Tampieri, F., Trombetti, F. and Grostra, U., 1992, "Dispersion Simulation of a Wind Tunnel Experiment with Lagrangian Particle Models," *Il Nuovo Cimento*, Vol. 15C, pp. 140~158.
- Anfossi, D., Ferrero, E., Brusasca, G., Marzorati, A. and Tinarelli, G., 1993, "A Simple Way of Computing Buoyant Plume Rise in Lagrangian Stochastic Dispersion Models," *Atmos. Environ.*, Vol. 27A, pp. 1443~1451.
- Briggs, G. A., 1975, "Lecture on Air Pollution and Environmental Impact Analysis," *American Meteorological Society*, Boston, MO.
- Brost, R. A. and Wynaard, J. C., 1978, "A Model Study of the Stably Planetary Boundary Layer," *J. Atmos. Sci.*, Vol. 35, pp. 1427~1440.
- Counihan, J., 1975, "Adiabatic Atmosphere Boundary Layers: A Review and Analysis of Data from the Period 1880~1972," *Atmos. Environ.*, Vol. 9, pp. 871~905.
- Craft, T. J., Launder, B. E. and Suga, K., 1997, "Prediction of Turbulent Transitional Phenomena with a Nonlinear Eddy-Viscosity Model," *Int. J. Heat Fluid Flow*, Vol. 18, pp. 15~28.
- Detering, H. W. and Etling, D., 1985, "Application of the  $E-\epsilon$  Turbulence Model to the Atmospheric Boundary Layer," *Boundary-Layer Meteorol.*, Vol. 36, pp. 201~209.
- Duykerke, P. G., 1988, "Application of the  $E-\epsilon$  Turbulence Closure Model to the Neutral and Stable Atmospheric Boundary Layer," *J. Atmos. Sci.*, Vol. 45, pp. 865~880.
- Etling, D., Reuss, J., Wamser, M., 1986, "Application of a Random Walk Model to Turbulent Diffusion in Complex Terrain," *Atmos. Environ.*, Vol. 20, pp. 741~747.
- Hug, P. and Stewart, E. J., 1999, "A Laboratory Study of Buoyant Plumes in Laminar and Turbulent Crossflows," *Atmos. Environ.*, Vol. 30, pp. 1125~1135.
- Kim, K. C., Kim, S. G. and Kim, B. C., 1997, "Pollutant Dispersion Behavior from Stack in Thermally Stratified Wind (II)," AFERC Research Report AFR-97-C04, Pohang University of Science and Technology, pp. 83-102.
- Kim, H. G. and Lee, C. M., 1998, "Pollutant Dispersion Over Two-Dimensional Hilly Terrain," *KSME Int. J.*, Vol. 12, No. 1, pp. 96~111.
- Kim, H. G. and Patel, V. C., 2000, "Test of Turbulence Models for Wind Flow over Terrain with Separation and Recirculation," *Boundary-Layer Meteorol.*, Vol. 94, pp. 5~21.
- Lu, Q. Q., 1995, "An Approach to Modeling Particle Motion in Turbulent Flows. I. Homogeneous, Isotropic Trubulence," *Atmos. Environ.*, Vol. 29, No. 3, pp. 423~436.
- Monin, A. S. and Obukhov, A. M., 1954, "Basic Regularity in Turbulent Mixing in the Surface Layer of the Atmosphere," *Trans. Geophys. Inst. Acad. Sci., U.S.S.R.*, Vol. 24, pp. 163~187.
- Raupach, M. R. and Legg, B. J., 1983, "Turbulent Dispersion from an Elevated Line Source: Measurements of Wind-Concentration Moments and Budgets," *J. Fluid Mech.*, Vol. 136, pp. 111~137.
- Thomson, D. J., 1987, "Criteria for the Selection of Stochastic Models of Particle Trajectories in Turbulent Flow," *J. Fluid Mech.*, Vol. 180, pp. 529~556.
- van Dop, H., Nieuwstadt, F. T. M. and Hunt, J. C. R., 1985, "Random Walk Models for Particle Displacements in Inhomogeneous Unsteady Turbulent Flows," *Phys. Fluids*, Vol. 28, pp. 1639~1653.
- Willis, G. E. and Deardorff, J. W., 1983, "On Plume Rise Within a Convective Boundary Layer," *Atmos. Environ.*, Vol. 17, pp. 2435-2447.